JACC: CLINICAL ELECTROPHYSIOLOGY VOL. 6, NO. 2, 2020

Validation of Dipole Density Mapping During Atrial Fibrillation and Sinus Rhythm in Human Left Atrium

Rui Shi, MD, PhD,[a,b] Paras Parikh, PhD,[c] Zhong Chen, MBBS, PhD,[b] Nathan Angel, PhD,[c] Mark Norman, MD,[b] Wajid Hussain, MD,[b] Charlie Butcher, MBBS,[b] Shouvik Haldar, MD,[b] David G. Jones, MD,[b] Omar Riad, MD,[b] Vias Markides, MD,[b] Tom Wong, MD[b]

ABSTRACT

OBJECTIVES This study sought to validate the accuracy of noncontact electrograms against contact electrograms in the left atrium during sinus rhythm (SR) and atrial fibrillation (AF).

BACKGROUND Noncontact mapping offers the opportunity to assess global cardiac activation in the chamber of interest. A novel noncontact mapping system, which records intracardiac voltage to derive cellular charge sources (dipole density), allows real-time mapping of AF to guide ablation.

METHODS Noncontact and contact unipolar electrogram pairs were recorded simultaneously from multiple locations. Morphology correlation and timing difference of reconstructed electrograms obtained from a noncontact catheter were compared with those from contact electrograms obtained from a contact catheter at the same endocardial locations.

RESULTS A total of 796 electrogram pairs in SR and 969 electrogram pairs in AF were compared from 20 patients with persistent AF. The median morphology correlation and timing difference (ms) in SR was 0.85 (interquartile range [IQR]: 0.71 to 0.94) and 6.4 ms (IQR: 2.6 to 17.1 ms); in AF was 0.79 (IQR: 0.69 to 0.88) and 14.4 ms (IQR: 6.7 to 26.2 ms), respectively. The correlation was stronger and the timing difference was less when the radial distance (r) from the noncontact catheter center to the endocardium was $\leq$ 40 versus $>$ 40 mm; 0.87 (IQR: 0.72 to 0.94) versus 0.73 (IQR: 0.56 to 0.88) and 5.7 ms (IQR: 2.6 to 15.4 ms) versus 15.1 ms (IQR: 4.1 to 27.7 ms); $p < 0.01$ when in SR; 0.81 (IQR: 0.69 to 0.89) versus 0.67 (IQR: 0.45 to 0.82) and 12.3 ms (IQR: 5.9 to 21.8 ms) versus 28.3 ms (IQR: 16.2 to 36.0 ms); $p < 0.01$ when in AF.

CONCLUSIONS This novel noncontact dipole density mapping system provides comparable reconstructed atrial electrogram measurements in SR or AF in human left atrium when the anatomical site of interest is $\leq$40 mm from the mapping catheter. (J Am Coll Cardiol EP 2020;6:171–81) © 2020 The Authors. Published by Elsevier on behalf of the American College of Cardiology Foundation. This is an open access article under the CC BY-NC-ND license (http://creativecommons.org/licenses/by-nc-nd/4.0/).

Understanding patient-specific non-pulmonary vein mechanisms in persistent atrial fibrillation (AF) is essential to establish effective ablation strategies that improve clinical outcomes. Sequential mapping of AF is challenging using conventional contact catheters given the continuously changing patterns of activation. The instantaneous and global nature of noncontact mapping may help to

From the [a]Department of Cardiovascular Medicine, The First Affiliated Hospital of Xi'an Jiaotong University, Xi'an, China; [b]Heart Rhythm Centre, The Royal Brompton and Harefield National Health Service Foundation Trust, National Heart and Lung Institute, Imperial College London, United Kingdom; and [c]Acutus Medical, Carlsbad, California. Dr. Shi has received a fellowship scholarship from the China Scholarship Council (No. 201606285148) paid to the institution. Drs. Parikh and Angel are employees of Acutus Medical, and both hold stock options. Dr. Markides has a consulting agreement with Biosense Webster. Dr. Wong has received support from National Institute for Health Research. All other authors have reported that they have no relationships relevant to the contents of this paper to disclose.

The authors attest they are in compliance with human studies committees and animal welfare regulations of the authors' institutions and Food and Drug Administration guidelines, including patient consent where appropriate. For more information, visit the *JACC: Clinical Electrophysiology* author instructions page.

Manuscript received January 22, 2019; revised manuscript received September 17, 2019, accepted September 19, 2019.

ISSN 2405-500X https://doi.org/10.1016/j.jacep.2019.09.012

ABBREVIATIONS AND ACRONYMS

AF = atrial fibrillation
IQR = interquartile range
LA = left atrium
LAA = left atrial appendage
SR = sinus rhythm

elucidate the underlying patient-specific mechanisms contributing to the perpetuation of AF (1,2).

A novel noncontact dipole density mapping system (Acutus Medical, Carlsbad, California) was designed to overcome some limitations of existing technologies and deliver improved temporal and spatial resolution (3). A double layer of dipole density (coulombs [C]/cm) forms during propagation that embodies the wave front and generates the cardiac potential field (volts). The fundamental differences between voltage and dipole density lie in both the averaging effect of "spatial summation" and in the volume of space occupied by each (4). Theoretically, dipole density-based mapping provides a more localized portrayal of activation patterns than voltage-based mapping does, with less far-field interference. However, validation of dipole density mapping in the human left atrium (LA) has not been previously reported.

SEE PAGE 182

The purpose of this study was to validate the accuracy of unipolar reconstructed electrograms by this dipole density-based noncontact mapping system against conventional contact electrograms obtained from a conventional circular catheter during sinus rhythm (SR) and AF in the human LA.

METHODS

STUDY POPULATION. This study included 20 consecutive patients with persistent AF who underwent an electrophysiologic study followed by radiofrequency catheter ablation guided by noncontact dipole density mapping. The written consent forms were signed by all patients before the procedure, and the study was approved by the national ethics committee (National Health Service Health Research Authority).

NONCONTACT DIPOLE DENSITY MAPPING AND VALIDATION DESIGN. The noncontact mapping catheter (AcQMap; Acutus Medical) has a 25-mm diameter spheroid-shape formed by 6 splines, with each containing 8 electrodes and 8 ultrasound transducers (**Central Illustration, Panel A**). The system reconstructs 3-dimensional endocardial anatomy from reflection points marked by ultrasound transducers. An impedance-based localization system tracks the position of electrodes, integrates ultrasound distances, and registers the acquired surface mesh within a unified coordinate system. Dipole density is inversely derived from the raw, unipolar cavitary electrograms sensed by the noncontact electrodes. Reconstructed electrograms are "forward-calculated" from the derived distribution of dipole density. In contrast to interpolation between points of measured data, inverse solutions predict data based on an appropriate model that fundamentally describes the behavior of the data. Ultimately, comparable models with low measurement noise can accurately predict values farther away from the locus of measurement points than approximate models with high measurement noise. The presence of measurement noise requires the application of regularization to prevent large-scale multiplication of noise into an erroneous prediction. These challenges and limitations apply to the present method under evaluation and are accordingly contained within the results.

An electric dipole consists of 2 oppositely charged particles separated by a small distance. When a myocardial cell is stimulated, ionic currents flow through membrane ion channels and a small dipolar imbalance in charge emerges in the adjoining extracellular medium. As propagation proceeds, the combined activation of cells forms a macroscopic double layer of dipole density, in units of C/cm, that physically embodies the wave front and generates the cardiac potential field, in units of volts (5). It is precisely this potential field that contact and noncontact electrodes sense. Charge density, itself, cannot be physically measured. Only its force (voltage) can be measured and, thus, dipole density must be inversely derived by a mathematical algorithm.

Four key stages of methodology affect the accuracy of this dipole density-based noncontact mapping system: 1) inputs to the inverse solution, including the noncontact, voltage-based electrograms and geometric coordinates of the electrodes and surface mesh; 2) mathematics of the inverse solution that derive dipole density; 3) post-processing of dipole density to reconstruct the unipolar, voltage-based electrograms on the anatomical surface; and 4) detection of local activation time for the display of wave front propagation from either dipole density or voltage. Methods of activation detection (methodology 4) and associated errors are known and common to all mapping technologies and are not examined in this study. However, the first 3 methodologies are unique to this mapping system and therefore constitute our scope of examination (see detailed explanation in the Online Methods 1 and 2). Because dipole density cannot be physically measured, it was not directly examined in this in vivo study. Accordingly, this validation was limited to examination of the reconstructed unipolar voltage. Specifically, the accuracy of this mapping system was assessed using cross-correlation to compare morphology and

CENTRAL ILLUSTRATION **Contact and Noncontact Catheters and Reconstructed Surface Mesh of the Left Atrium**

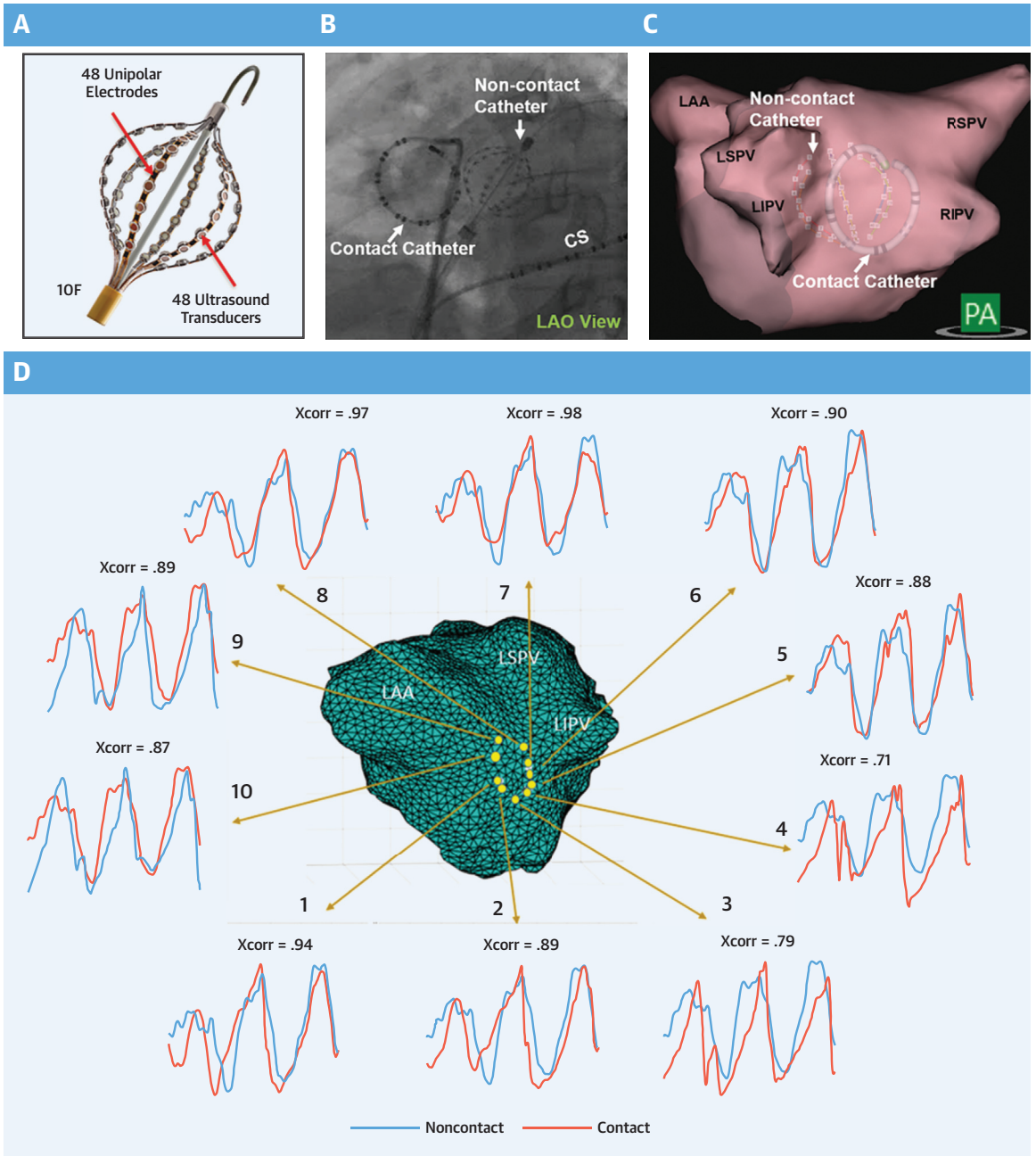

Shi, R. et al. J Am Coll Cardiol EP. 2020;6(2):171–81.

(A) Depiction of the noncontact catheter with 6 splines, each carrying 8 ultrasound transducers and 8 high-fidelity unipolar electrodes. **(B)** Noncontact catheter and circular contact catheter in the left atrium (LA) (left anterior oblique [LAO] view). **(C)** LA anatomy constructed by the noncontact catheter mapping system (poster-oanterior [PA] view). The noncontact mapping catheter is shown in the center of the LA chamber and the contact circular mapping catheter is positioned on the posterior wall. **(D)** Morphology comparison, cross-correlation (Xcorr), of 10 noncontact reconstructed and contact electrogram pairs. The **yellow dots** represent 10 locations of the circular contact mapping electrodes with the relevant paired contact **(red)**/noncontact **(blue)** electrogram. CS = coronary sinus; LAA = left atrial appendage; LIPV = left inferior pulmonary vein; LSPV = left superior pulmonary vein; RIPV = right inferior pulmonary vein; RSPV = right superior pulmonary vein.

TABLE 1 The Median Morphology Correlation (Cross-Correlation) and Timing Difference Between Contact and Noncontact Electrograms in SR and AF

	Sinus Rhythm		Atrial Fibrillation	
	Correlation	Timing Difference	Correlation	Timing Difference
N = 20	0.85 (0.71–0.94)	6.4 (2.6–17.1)	0.79 (0.69–0.88)	14.4 (6.7–26.2)
Radial distance (r) from center of noncontact catheter				
≤40 mm	0.87 (0.72–0.94)	5.7 (2.6–15.4)	0.81 (0.69–0.89)	12.3 (5.9–21.8)
>40 mm	0.73 (0.56–0.88)	15.1 (4.1–27.7)	0.67 (0.45–0.82)	28.3 (16.2–36.0)
p Value	<0.01	<0.01	<0.01	<0.01
Orientation to noncontact catheter				
Polar	0.81 (0.67–0.92)	8.64 (3.84–19.4)	0.80 (0.69–0.88)	16.6 (8.2–30.1)
Equatorial	0.85 (0.73–0.95)	5.44 (2.24–15.4)	0.81 (0.69–0.89)	13.3 (6.0–24.0)
p Value	0.001	<0.01	0.28	<0.01

Values are median (interquartile range). Timing difference is expressed in ms.
AF = atrial fibrillation; SR = sinus rhythm.

timing of reconstructed voltage-based electrograms, post-processed from the dipole density-based inverse solution, to contact electrograms, measured from a conventional circular catheter, at the same locations across the LA endocardial surface.

ELECTROPHYSIOLOGY STUDY AND ELECTROANATOMIC MAPPING PROCEDURES. Clinical application of noncontact dipole density mapping has been described in detail previously (4). Specific to this study, a standard decapolar contact catheter was placed in the coronary sinus and a quadripolar catheter was placed in the inferior vena cava below the level of the diaphragm, with 1 electrode used as an electrical reference for unipolar recording. The LA was accessed via double trans-septal punctures. The noncontact catheter and 20-pole circular catheter (Inquiry Optima; Irvine Biomedical, Inc., Abbott Laboratories, Irvine, California) with 2-mm electrodes, 15- to 25-mm variable loop radii were introduced into the LA via a 16-F steerable trans-septal sheath (AcQGuide, Acutus Medical) for recording and mapping. Heparin was administered by intravenous bolus to maintain an activated clotting time ≥350 s to prevent thrombus formation. The noncontact catheter was fully deployed over a 0.032-inch guidewire, after having been positioned in the middle of the LA for both acquisition of endocardial anatomy and recording cardiac activation (**Central Illustration, Panel B**).

DATA ACQUISITION. By maneuvering and rotating the deployed noncontact catheter, ultrasonic reflections were detected and processed to reconstruct the atrial chamber anatomy. With the deployed noncontact catheter positioned in the center of the LA, a conventional circular catheter was navigated to 7 pre-specified regions in the LA for simultaneous recording of contact and noncontact unipolar electrograms on the septum; roof; floor; left atrial appendage (LAA); and the lateral, anterior, and posterior walls (**Central Illustration, Panel C**). The noncontact mapping catheter in its fully deployed state was positioned and rotated within the atrial chamber without direct contact with the atrial endocardium when creating the anatomy of the LA. The noncontact mapping catheter was positioned generally in the center of the chamber when performing the electrical mapping. There is no requirement to hold the AcQMap catheter in a fixed position, as the AcQMap system continuously tracks the position of the catheter spline electrodes and inputs the associated coordinates for each instant of inverse calculation. Comparisons of contact and reconstructed electrograms were thereby made from multiple recordings at those 7 pre-specified regions during SR and AF.

All recorded segments of AF and SR were captured for a duration of 30 s and were reviewed and analyzed off-line. SR was restored either by catheter ablation or external cardioversion, if required. The AcQMap methodology applies an algorithm to determine local activation time and organizes activation time as a moving window of isochronal timing, called a propagation history map (5).

VALIDATION AND ACCURACY METHODS. Data analysis. Data including the coordinates of surface mesh points, localized contact and noncontact catheter electrodes, and all associated unipolar electrograms were exported for off-line analyses using custom MATLAB scripts (MathWorks, Natick, Massachusetts). For AF recordings, 300- to 600-ms segments containing multiple cycles were selected for analysis, whereas single-atrial deflections were selected for SR recordings. All segments were manually chosen to ensure complete exclusion of QRS waves and T waves.

FIGURE 1 **Morphology Correlation, Timing Difference, and RMS Amplitude During Sinus Rhythm**

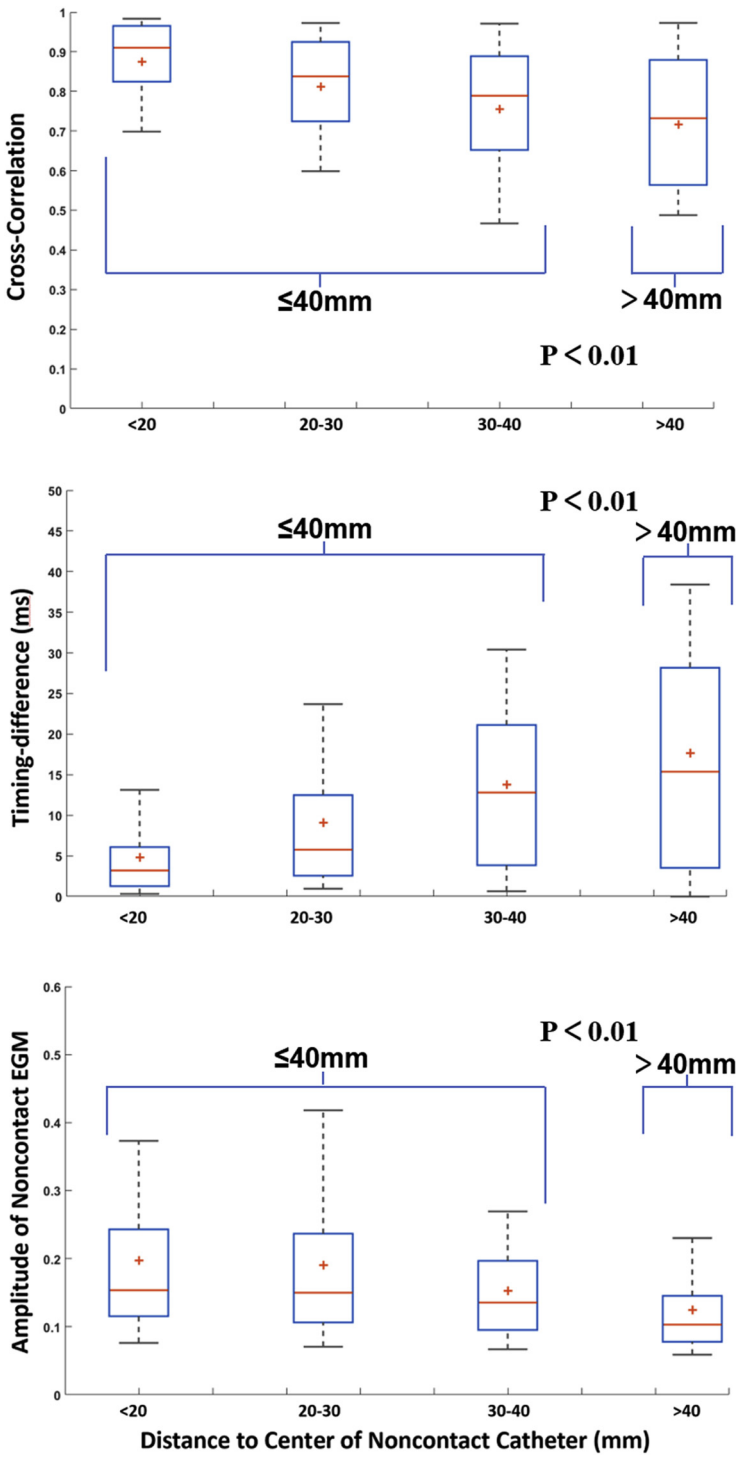

Effects of distance from the noncontact catheter center to the endocardial comparison sites on morphology correlation **(upper)**, timing difference **(middle)**, and root-mean-square (RMS) amplitude **(lower)** between unipolar reconstructed noncontact and contact electrogram pairs during sinus rhythm. The box plot illustrates the median with interquartile range. The **red** + **sign** illustrates the arithmetic mean and the whiskers depict the 5th and 95th percentiles.

Correspondence between noncontact reconstructed and contact electrograms was evaluated using the mean-subtracted cross-correlation (see detailed explanation in the Online Methods 3). In addition, the root-mean-square value of each of the selected segments were calculated for the electrogram pairs obtained during SR. Amplitude was not calculated and compared for AF segments due to the dramatic variation in amplitude over time. In contrast, SR is an inherently regular rhythm with consistent and repeatable amplitude measures that are appropriate for analysis. Metrics comparing noncontact to contact electrograms have been previously described (6,7).

Each mapping catheter electrode was indexed to a specific geodesic vertex on the anatomy. Cross-correlation was then calculated at each surface-mesh vertex residing within 5 mm from the index vertex. The maximum correlation value found within this 5-mm radius was assigned as the morphology match value for that contact and noncontact electrogram pairs. This radius accounted for inverse-solution and electrode-localization errors and ensured the most relevant morphologic assessment. Factors including contact catheter distance from the anatomy, stability of mapping catheter localization, and baseline noise were examined to achieve appropriate comparisons of electrical data.

STATISTICAL METHODS. The data was pooled across all patients as a single rhythm group, for both SR and AF. Analysis of morphology was done by using the standard cross-correlation metric. Pearson correlation is calculated across the time series for each sample offset, and a set of Pearson correlation values are thereby accrued. Cross-correlation is defined as the maximum correlation value obtained within the accrued set of values. Timing difference is defined as the time difference associated with sample offset required to achieve cross-correlation. These 2 metrics were calculated, individually, for every location of all contact electrodes and were accumulated into a population of independent morphology and timing measures. Continuous and normally distributed data were presented as mean ± SD, and an independent Student's *t*-test was used to test differences between 2 groups. Normally distributed data were expressed as median (interquartile range [IQR]) and compared using the non-parametric Mann-Whitney *U* test. Statistical calculations were made in SPSS version 22.0 (IBM Corp., Armonk, New York). The results were considered significant for a p value < 0.05.

RESULTS

PATIENTS. Twenty patients (mean age 64 ± 12 years, 14 male) with persistent AF (mean AF duration 9 ± 6 months) were studied. The mean LA parasternal long-axis diameter was 43 ± 5 mm and left ventricular ejection fraction was 49 ± 14% (see detailed patients' characteristics in Online Table 1).

VALIDATION OF RECONSTRUCTED ELECTROGRAMS IN SR. A total of 796 SR electrogram pairs were compared, with results summarized in **Table 1**. Median morphology cross-correlation and timing difference was 0.85 (IQR: 0.71, 0.94) and 6.4 ms (IQR: 2.6, 17.1), respectively. Morphology correlation and timing difference as a function of distance from the center of the noncontact catheter during SR are summarized in **Figure 1**. Both the morphology correlation and timing difference of electrogram pairs improved when the radial distance (r) between the endocardial comparison site and the center of the noncontact catheter was ≤40 mm, with 91.5% of the sites located within this range. As shown in **Figure 1**, median morphology correlation was 0.87 (IQR: 0.72 to 0.94) versus 0.73 (IQR: 0.56 to 0.88); $p < 0.01$ and timing difference was 5.7 ms (IQR: 2.6 to 15.4 ms) versus 15.1 ms (IQR: 4.1 to 27.7 ms); $p < 0.01$ for $r \leq 40$ mm versus $r > 40$ mm, respectively. Electrogram pairs at equatorial sites had a significantly greater correlation than at polar sites: median: 0.85 (IQR: 0.73 to 0.95) versus 0.81 (IQR: 0.67 to 0.92); $p = 0.01$. However, polar sites were significantly farther from the center of the noncontact catheter: median: 32.0 mm (IQR: 24.7 to 40.2 mm) versus 28.0 mm (IQR: 21 to 33.6 mm); $p < 0.01$.

The amplitude of contact electrograms in SR increased as the contact catheter was moved closer to the endocardial surface and farther in radial distance from the center of the noncontact catheter: median: 0.22 mV (IQR: 0.14 to 0.40 mV) versus 0.35 mV (IQR: 0.22 to 0.46 mV); $p < 0.01$ for $r \leq 40$ mm versus $r >$ 40 mm, respectively. Conversely, the amplitude of corresponding non-contact-reconstructed electrograms decreased: median: 0.15 mV (IQR: 0.10 to 0.22 mV) versus 0.10 mV (IQR: 0.08 to 0.14 mV); $p < 0.01$ for $r \leq 40$ mm versus $r > 40$ mm, respectively. Endocardial sites for which the amplitudes of electrogram pairs were closely matched were located closer to the center of the noncontact catheter: median: 21.2 mm (IQR: 16.2 to 30.2 mm) versus 28.4 mm (IQR: 23.2 to 35.2 mm); $p < 0.01$ for root-mean-square amplitude ratio ≥ 0.9 versus < 0.9, respectively. These sites also had a correspondingly better morphology correlation: median: 0.94 (IQR: 0.83 to 0.98) versus. 0.80 (IQR: 0.67 to 0.90); $p < 0.01$. As a

FIGURE 2 Morphology Correlation and Timing Difference During AF

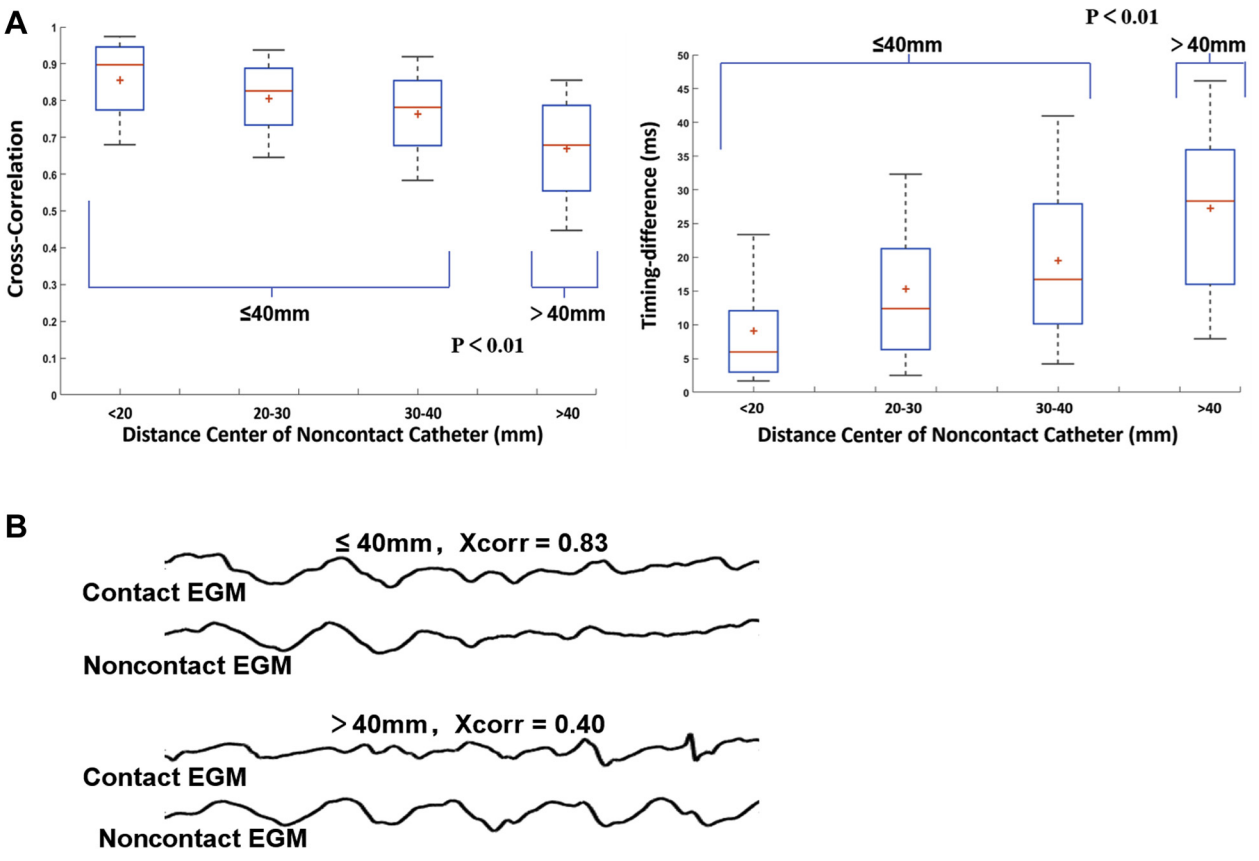

(A) Box plots show the effects of distance from the noncontact catheter center to the endocardial comparison sites on cross-correlation (Xcorr) **(left)** and timing difference **(right)** between reconstructed unipolar noncontact and contact electrogram (EGM) pairs during atrial fibrillation (AF). **(B)** This example demonstrates poor morphology correlation with AF electrogram pairs at a site >40 mm from center of the noncontact mapping catheter. (See Figure 1 for details of the figure annotations.)

general observation, noncontact-reconstructed electrograms with the lowest amplitudes were observed at sites furthest from the center of the noncontact catheter (Figure 1).

VALIDATION OF RECONSTRUCTED ELECTROGRAMS IN AF. A total of 969 AF electrogram pairs were compared, with results summarized in Table 1. Median morphology correlation and timing difference were 0.79 (IQR: 0.69 to 0.88) and 14.4 ms (IQR: 6.7 to 26.2), respectively. Central Illustration, Panel D illustrates an example of a dataset comparing 10 pairs of non-contact-reconstructed electrograms (red waveform) to the corresponding contact electrograms (blue waveform) on the lateral wall of LA.

Similar to observations in SR, morphology correlation and timing difference of AF electrogram pairs improved when the radial distance between the endocardial comparison site and the center of the noncontact catheter was ≤40 mm, with 85% of the sites located within this range (Table 1). As shown in Figure 2, median morphology correlation was 0.81 (IQR: 0.69 to 0.89) versus 0.67 (IQR: 0.45 to 0.82); $p < 0.01$ and median timing difference was 12.3 ms (IQR: 5.9 to 21.8 ms) versus 28.3 ms (IQR: 16.2 to 36.0 ms); $p < 0.01$ for $r \leq 40$ mm versus $r > 40$ mm, respectively. Electrogram pairs at equatorial and polar sites had the essentially the same morphology correlation: median: 0.80 (IQR: 0.69 to 0.88) versus 0.81 (IQR: 0.69 to 0.89); $p = 0.28$. However, timing differences for equatorial and polar sites were significantly different: median: 16.6 ms (IQR: 8.2 to 30.1 ms) versus 13.3 ms (IQR: 6.0 to 24.0 ms); $p < 0.01$.

Morphology correlation and timing difference at the specific regions of the LA for AF are shown in Figure 3. The regions with the highest median morphology correlation were observed on the roof: 0.87 (IQR: 0.77 to 0.91), and posterior wall: 0.86

FIGURE 3 Morphology Correlation and Timing Difference for Specific Regions of the LA During Atrial Fibrillation

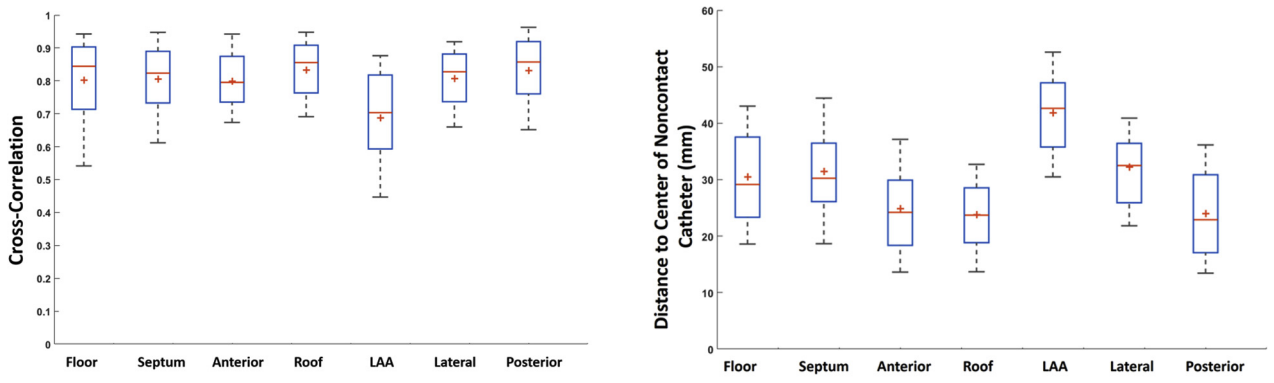

The roof and posterior wall have the highest correlation. The left atrial appendage (LAA), being the furthest away from the noncontact catheter center, has the lowest correlation. (See Figure 1 for details of the figure annotations.)

(IQR: 0.76 to 0.90). The region with the lowest morphology correlation was within and near the LAA ostium: median: 0.70 (IQR: 0.59 to 0.81). Of note, the LAA region was also the furthest from the center of the noncontact catheter: median: 39 mm (IQR: 31 to 51 mm).

DISCUSSION

MAIN FINDINGS. This is the first study to compare dipole density-based reconstructed unipolar electrograms with contact electrograms in the human LA. This signifies the first quantitative step in validating dipole density-based mapping using physically comparable measurements. Morphology correlation and timing difference values were significantly improved at radial distances ≤40 mm, with most of the comparison sites located within this range (more than 85% in this evaluation).

PREVIOUS VALIDATION STUDY OF NONCONTACT MAPPING. The global, noncontact mapping mode of the EnSite System (Abbott Laboratories, St. Paul, Minnesota) established a new concept in the history of 3-dimensional mapping, as shown by previous studies (8,9). Earley et al. (6) compared the contact unipolar electrograms with noncontact "virtual" unipolar electrograms by using the noncontact EnSite Array catheter in the human LA during SR and AF. LA electrograms correlated well (0.81) during SR. However, the cross-correlation values in AF dropped from 0.72 to 0.59 when ventricular far-field signals were excluded from correlation analysis by inducing temporary atrioventricular block with adenosine. This implied that the common-mode ventricular component of the unipolar electrogram may have contributed a favorable bias in the assessment of the EnSite system, with an associated overestimation of its accuracy in mapping AF (6). Differences exist between the present study and the data reported by Earley et al. (6). In their assessment of AF, the QRS complex was included in the signal morphology over a duration of approximately 7 s. Inclusion of the QRS complex artificially improves the timing difference, as the far-field QRS complex is inherently well-aligned in time across all measurements and reconstructions, and this feature dominates the determination of timing difference. In contrast, the present assessment methodology did not include the QRS complexes. Instead, a multitude of shorter-duration signals were compared for time segments between, and not including, QRS complexes. A stronger cross-correlation (0.85 and 0.79) was shown in SR and AF, respectively. This supports the view that dipole density-based mapping can be used to detect endocardial activity of AF with increased accuracy (3).

An inherent limitation of noncontact mapping is that the morphology correlation is dependent on the distance between the noncontact mapping catheter and the endocardial wall. In the validation studies using the EnSite Array catheter, Earley et al. (6) and Lin et al. (10) reported a significant decrease in morphology correlation for endocardial points >40 mm and >38 mm from the center of the array, respectively. Those studies also indicated greater variation in the morphology correlation and timing difference for specific regions of the LA, such as the more distant LAA and mitral-annular sites (6,10). In the present validation study, the distance from the center of the noncontact catheter to the endocardial

wall also imposed a similar limitation on the accuracy and precision of voltage-based measurement. However, the results showed good accuracy and precision (correlation 0.79 in AF) with ventricular complexes excluded from the calculation of cross-correlation.

Independent from morphology correlation, electrogram timing is also an important metric of evaluation (10). In this study, timing difference gradually increased with increasing distance between the center of the noncontact catheter and the endocardial comparison sites. Timing accuracy is known to be affected by complex geometry, such as the shape of the appendage and venous antra (11). Timing errors are imposed in different ways on both the noncontact-reconstructed and contact electrograms from the complex geometric shape of LA anatomy and from propagating wave fronts having a "sharp" curvature. Delay caused by catheter tissue contact presents another known dimension of variation in comparing noncontact and contact electrogram timing. Such geometric- and tissue-pressure-related factors were not specifically evaluated in this study. Nonetheless, such factors are inherent within these reported results. Electrogram comparison in this study methodology does not rely on phase for measurement of activation times. Phase calculation is not performed for any purpose in the AcQMap algorithms or in the comparison analysis. Consequently, phase discontinuity does not manifest as a limitation in the present study.

CLINICAL IMPLICATION. There are 2 steps to manipulate the noncontact mapping catheter during the procedure: 1) to create the atrial anatomy; and 2) to acquire the electrical data.

1. The mapping catheter was positioned within the atrial chamber in its fully deployed state and was then rotated and translated within the chamber to close proximity but not in direct contact with the endocardium to reconstruct the atrial anatomy.
2. The catheter was then positioned generally in the center of the chamber for performing the electrical mapping. It is not necessary to "hold" the catheter in a fixed position. The system localizes the electrodes positions in real time; and their coordinates are applied in the inverse algorithm for every instant of calculation. The signals associated with electrodes located within 5 mm of the endocardial surface were automatically rejected by the algorithm to maintain the integrity of noncontact mapping processing.

This novel noncontact dipole density mapping system harnesses the advantage of reconstructing an anatomy generated by high-spatial resolution ultrasound and deriving dipole density that provides more localized maps of cardiac conduction than voltage (5). Non-pulmonary vein triggers and specific substrate conditions have become decisively relevant in treating persistent AF. Technologies are evolving toward localization of targets for ablation outside the pulmonary veins (1,12–15). Contact mapping technologies have limitations of either low-spatial resolution "global" or high-resolution sequential (regional) acquisition of data points. Technologies using phase algorithms may lead to a false-positive bias in detecting rotational activities and focal sources (16). Dipole density mapping addresses some of the limitations of conventional mapping and may contribute to uncovering the mechanisms of AF that remain to be fully elucidated.

We have shown in this study that noncontact electrograms collected by dipole density-based mapping are reliable in morphology correlation and timing difference within a radial distance of 40 mm from the center of the noncontact catheter. The resulting morphology correlation between noncontact and contact electrograms was the least at the LAA, which was usually the furthest distance from the center of the catheter splines than the rest of the atrial anatomy. Thus, the noncontact electrograms and cardiac conduction maps by dipole density mapping during AF must be interpreted with caution if anatomical areas are over 40 mm from the center of the noncontact catheter, such as in the region of the LAA. In practical terms, it is advisable for the novel noncontact catheter to be placed generally in the middle of the LA chamber during mapping. In doing so, it is likely that the majority of endocardial aspects of the LA will be within optimal range.

STUDY LIMITATIONS. First, dipole (charge) density is an electrical entity that cannot, itself, be directly measured by contact mapping, although charges and voltages are inherently linked. Accordingly, this study was limited to comparing post-processed voltage-based electrograms to corresponding contact electrograms at the same location on the chamber wall. The reconstructed noncontact electrograms therefore have the associated inherent limitations from its derivation methodology and the inherent reproduction of far-field blending. Second, validation analysis was limited to segments within the R-R intervals to avoid interference from ventricular electrograms. The associated short duration of compared sample sets would impose some limitations on evaluation of activation stability in both the time domain and in phase space. Consequently,

evaluation of stability was not within the scope of this validation. Third, the study did not assess the impact of anatomical geometry on measurement locations that were either within or adjacent to the direct field-of-view of the noncontact catheter on the accuracy of data collection. The data presented in the present study includes comparison of signals recorded and reconstructed during AF. We propose that the data presented would be predictive of a future study that could be contemplated using bipolar signals, in addition to unipolar signals, to validate the accuracy of complex fractionated atrial electrograms.

CONCLUSIONS

This novel noncontact dipole density mapping system provides comparable reconstructed atrial electrogram measurements in SR or AF in human LA when the anatomical site of interest is ≤40 mm from the mapping catheter.

ACKNOWLEDGMENT The authors wish to acknowledge and thank Xinwei Shi, PhD, and Min Zhu, PhD (algorithm scientists at Acutus Medical, Inc.) for their contributions to the analytic methodology.

ADDRESS FOR CORRESPONDENCE: Dr. Tom Wong, Heart Rhythm Centre, The Royal Brompton and Harefield National Health Service Foundation Trust, National Heart and Lung Institute, Imperial College London, Sydney Street, London SW3 6NP, United Kingdom. E-mail: t.wong2@rbht.nhs.uk.

PERSPECTIVES

COMPETENCY IN MEDICAL KNOWLEDGE: This novel noncontact dipole density mapping system harnesses the advantage of reconstructing an anatomy generated by high-spatial resolution ultrasound and deriving dipole density that provides more localized maps of cardiac conduction than voltage. Noncontact electrograms collected by dipole density–based mapping are reliable in morphology correlation and timing difference within a radial distance of 40 mm from the center of the noncontact catheter. Thus, the noncontact electrograms and cardiac conduction maps by dipole density mapping during AF must be interpreted with caution if anatomical areas are over 40 mm from the center of the noncontact catheter.

TRANSLATIONAL OUTLOOK: Nonpulmonary vein triggers and specific substrate conditions have become decisively relevant in treating persistent AF. Contact mapping technologies have limitations of either low-spatial resolution "global" or high-resolution sequential (regional) acquisition of data points. Technologies using phase algorithms may lead to a false-positive bias in detecting rotational activities and focal sources. Dipole density mapping fundamentally addresses these limitations and may contribute to uncovering the mechanisms of AF which has thus far been a challenging quest.

REFERENCES

1. Haissaguerre M, Hocini M, Denis A, et al. Driver domains in persistent atrial fibrillation. Circulation 2014;130:530–8.

2. Yamaguchi T, Tsuchiya T, Miyamoto K, Nagamoto Y, Takahashi N. Characterization of non-pulmonary vein foci with an EnSite array in patients with paroxysmal atrial fibrillation. Europace 2010;12:1698–706.

3. Grace A, Verma A, Willems S. Dipole density mapping of atrial fibrillation. Eur Heart J 2017;38:5–9.

4. Shi R, Norman M, Chen Z, Wong T. Individualized ablation strategy guided by live simultaneous global mapping to treat persistent atrial fibrillation. Future Cardiol 2018;14:237–49.

5. Grace A, Willems S, Meyer C, et al. High-resolution noncontact charge-density mapping of endocardial activation. JCI Insight 2019;4:126422.

6. Earley MJ, Abrams DJ, Sporton SC, Schilling RJ. Validation of the noncontact mapping system in the left atrium during permanent atrial fibrillation and sinus rhythm. J Am Coll Cardiol 2006;48:485–91.

7. Bear LR, LeGrice IJ, Sands GB, et al. How accurate is inverse electrocardiographic mapping? A systematic in vivo evaluation. Circ Arrhythm Electrophysiol 2018;11:e006108.

8. Markides V, Schilling RJ, Ho SY, Chow AW, Davies DW, Peters NS. Characterization of left atrial activation in the intact human heart. Circulation 2003;107:733–9.

9. Weber S, Ndrepepa G, Schneider M, et al. Characterization of onset mechanism and waveform analysis in patients with atrial fibrillation using a high-resolution noncontact mapping system. J Cardiovasc Electrophysiol 2003;14:176–81.

10. Lin YJ, Higa S, Kao T, et al. Validation of the frequency spectra obtained from the noncontact unipolar electrograms during atrial fibrillation. J Cardiovasc Electrophysiol 2007;18:1147–53.

11. Steinhaus BM. Estimating cardiac transmembrane activation and recovery times from unipolar and bipolar extracellular electrograms: a simulation study. Circ Res 1989;64:449–62.

12. Cuculich PS, Wang Y, Lindsay BD, et al. Noninvasive characterization of epicardial activation in humans with diverse atrial fibrillation patterns. Circulation 2010;122:1364–72.

13. Pandit SV, Jalife J. Rotors and the dynamics of cardiac fibrillation. Circ Res 2013;112:849–62.

14. Narayan SM, Krummen DE, Rappel WJ. Clinical mapping approach to diagnose electrical rotors and focal impulse sources for human atrial fibrillation. J Cardiovasc Electrophysiol 2012;23:447–54.

15. Narayan SM, Baykaner T, Clopton P, et al. Ablation of rotor and focal sources reduces late recurrence of atrial fibrillation compared with trigger ablation alone: extended follow-up of the CONFIRM trial (Conventional Ablation for Atrial Fibrillation With or Without Focal Impulse and Rotor Modulation). J Am Coll Cardiol 2014;63:1761–8.

16. Allessie M, de Groot N. CrossTalk opposing view: rotors have not been demonstrated to be the drivers of atrial fibrillation. J Physiol 2014;592:3167–70.

KEY WORDS atrial fibrillation, accuracy, contact mapping, noncontact dipole density mapping, unipolar signal, validation

APPENDIX For an expanded Methods section and a supplemental table, please see the online version of this paper.